Molecular Organization and Dynamics of 1-Palmitoyl-2-oleoylphosphatidylcholine Bilayers Containing a Transmembrane α -Helical Peptide[†]

Witold K. Subczynski,*,^{‡,§} Ruthven N. A. H. Lewis,^{||} Ronald N. McElhaney,^{||} Robert S. Hodges,^{||,⊥} James S. Hyde,[§] and Akihiro Kusumi*,[∇]

Biophysics Department, Institute of Molecular Biology, Jagiellonian University, Al. Mickiewicza 3, 31-120 Krakow, Poland, Biophysics Research Institute, Medical College of Wisconsin, 8701 Watertown Plank Road, Milwaukee, Wisconsin 53226, Department of Biochemistry and MRC Group in Protein Structure and Function, University of Alberta, Edmonton, Alberta, Canada T6G 2H7, and Department of Biological Science, Graduate School of Science, Nagoya University, Chikusa-ku, Nagoya 464, Japan

Received August 28, 1997; Revised Manuscript Received November 11, 1997

ABSTRACT: The molecular organization and dynamics have been investigated in membranes consisting of 1-palmitoyl-2-oleoyl-L-α-phosphatidylcholine (POPC) and various ratios of a transmembrane α-helical peptide, Ac-K₂L₂₄K₂-amide (L24), in order to gain insights into how the transmembrane portions of membrane proteins are mixed with phospholipids and organized in biological membranes. Particular attention was paid to membranes with high peptide concentrations. The molecular organization and dynamics were studied in the ps-to-us regime using various spin-labeling techniques. Conventional ESR spectra as well as saturation-recovery curves measured in both the presence and the absence of molecular oxygen showed that phosphatidylcholine spin-labels detect the existence of a single homogeneous environment, indicating that both L24 and POPC are likely to be undergoing fast translational diffusion in L24-POPC membranes of up to 9 mol % peptide. Since 16-18 molecules of phosphatidylcholine are required to surround a transmembrane α-helical peptide [Morrow, M. R., Huschilt, J. C., and Davis, J. H. (1985) Biochemistry 24, 5396–5406], L24 must form L24-rich regions at a P/L ratio of 1/10 instantaneously. However, these results suggest that the lipid exchange rates among the bulk, boundary, and L24-rich regions are fast, and that the L24-rich regions must be forming and dispersing rapidly in a time scale shorter than 0.1 us, the conventional ESR spin-label time scale and the electron spin-lattice relaxation time scale in the presence of molecular oxygen. Although this does not exclude the possibility of the formation of small, stable oligomers of L24, it is unlikely because L24 lacks features that would favor their formation. L24 (9 mol %) increases the hydrophobicity of the central part of the POPC membrane from the level of 1-decanol to that of pure hexane and also increases the hydrophobicity near the membrane surface from the level of 2-propanol to that of 1-decanol. The effect of 9 mol % L24 on the order parameter profile is similar to that of decreasing the temperature by ~8 °C between 10 and 55 °C. It is concluded that L24 is highly miscible in POPC membranes even at high concentrations in the membrane.

Biological membranes are crowded with integral membrane proteins, and many biological membranes contain functional domains that are rich in membrane proteins and possess very small amounts of bulk lipids (1). However, we have a very limited understanding of the molecular organization and dynamics for membranes containing high concentrations of membrane proteins and protein-rich do-

mains (2 and references therein). In protein-rich domains, lipid molecules are always in contact with one or more protein molecules, and protein—protein contacts are common occurrences (1, 3). Therefore, the fluid-mosaic model (4), in which membrane proteins are floating in a sea of excess lipids, is not applicable and may even be misleading in understanding molecular organization and dynamics of protein-rich domains.

In the present investigation, we have studied the molecular organization and dynamics of 1-palmitoyl-2-oleoyl-L- α -phosphatidylcholine (POPC) 1 bilayers containing various quantities of a transmembrane α -helical peptide, $Ac-K_2L_{24}K_2$ -amide (L24). This peptide, like its parent peptide P_{24} , is designed such that the central polyleucine segment will form a stable α -helix which will partition into hydrophobic core of lipid bilayers with the charged and somewhat polar terminal lysine residues anchoring the ends of the peptide to the bilayer surface and inhibiting lateral aggregation of

[†] This work was supported in part by U.S. Public Health Services Grants GM27665, GM22923, and RR01008 awarded by NIH, an operating grant from the Medical Research Council of Canada (R.N.M.), and grants-in-aid from Jagiellonian University and the Ministry of Education of the Japanese government (A.K.).

^{*} Authors to whom correspondence should be addressed (W.K.S. at subczyn@mcw.edu; A.K. at akusumi@bio.nagoya-u.ac.jp).

[‡] Jagiellonian University.

[§] Medical College of Wisconsin.

Department of Biochemistry, University of Alberta.

¹MRC Group in Protein Structure and Function, University of Alberta.

[∇] Nagoya University.

the peptide via mutual charge repulsion (5). Indeed, a wide variety of approaches have shown that this family of peptides does form very stable α -helices that insert into phosphatidylcholine (PC) and phosphatidylethanolamine (PE) model membranes perpendicular to the bilayer plane with the N-and C-termini exposed to the aqueous environment near the bilayer surface (5–17).

When incorporated into PC model membranes, P24 alters the conformation of the lipid hydrocarbon chains in contact with the peptide so as to minimize the extent of mismatch between the hydrophobic length of the peptide and the host lipid bilayer (12-15), although this is not the case in PE bilayers (16). Moreover, in both PC and PE bilayers, P₂₄ (12, 13, 16) and related peptides (14, 15) also appear to alter the length of their α -helices slightly to accommodate any mismatch between the hydrophobic length of the peptide and the hydrophobic thickness of the bilayer. The compositional and structural simplicity of L24 and related peptides, and their predictable and well-characterized behavior in lipid bilayers, makes them excellent model compounds for fundamental studies of the effects of the transmembrane portions of natural membrane proteins on the organization and dynamics of the host lipid bilayer.

In this study, we are particularly concerned with how α -helical peptides are packed and organized in the membrane at high peptide concentrations. The molecular organization and dynamics were investigated in the ps-to- μ s regime, using various spin-labeling techniques. We studied (1) the alkyl chain order in the 100 ns time regime, (2) the effective reorientation time of the alkyl chains in the time regime between 10 ps and 10 ns, (3) the hydrophobicity profiles across the membrane, and (4) the local diffusion—solubility characteristics of oxygen molecules (oxygen transport parameter)² in the membrane, which are sensitive to the molecular dynamics up to several μ s.

In our previous studies of oxygen transport, molecular oxygen was used as a probe to study three-dimensional molecular organization and dynamics in membranes (2, 18-21). The rates of bimolecular collisions between oxygen and nitroxide spin-labels placed at specific locations in the membrane have been evaluated from the spin-lattice relaxation times $(T_1$'s) of spin-labels using a pulse ESR technique. Molecular oxygen has a unique characteristic as a membrane probe; its small size and appropriate level of hydrophobicity allow it to enter the small vacant pockets that are transiently formed in the membrane. Therefore, the bimolecular collision rate is sensitive to the dynamics of *gauche-trans* isomerization of lipid alkyl chains and to the structural nonconformability of neighboring lipids (2, 19, 20, 22).

In reconstituted membranes of bacteriorhodopsin (BR; 2) and dimyristoyl-L-α-phosphatidylcholine (DMPC) at a ratio of 1:80, in which BR exists as monomers, using molecular oxygen as a probe, the lipid environment was found to be homogeneous on a microsecond scale, the time scale defined by the spin-label T_1 . This finding supports the hypothesis that the lipid exchange rate between the bulk and the boundary regions is greater than the spin-lattice relaxation rate ($\sim 10^6 \, \mathrm{s}^{-1}$). In the BR reconstituted membrane at a ratio of 1:40, in which bacteriorhodopsin exists as 25% monomers and 75% trimers + oligomers of trimers (but not large aggregates), the presence of a special lipid environment was found where oxygen transport is five times slower than in the bulk + boundary region. This slow oxygen-transport domain (SLOT domain) is likely to be a self-associated BR domain. The residence time of the lipids in the slow oxygentransport domain was longer than 10^{-6} s, T_1 in the presence of 100% air. It was speculated that the SLOT domain consists of lipids in contact with two proteins and/or lipids in contact with protein and boundary lipids. It follows that the alkyl chains and BR are closely packed in the SLOT domain, with few vacant pockets to allow the entrance and movement of even small molecules such as molecular oxygen. It was concluded that molecular oxygen makes a particularly useful probe to study the molecular organization in protein-rich membranes. In this study, we paid special attention to whether or not such a SLOT domain exists in a membrane containing high concentrations of single transmembrane α -helices.

EXPERIMENTAL PROCEDURES

Materials. POPC and 1-palmitoyl-2-(n-doxylstearoyl)-L- α -phosphatidylcholine (n-PC, where n=5, 7, 10, 12, and 16) were from Avanti Polar Chemicals (Birmingham, AL). Tempocholine dipalmitoylphosphatidic acid ester (Tempo-PC) was a generous gift from Dr. S. Ohnishi (Kyoto University, Kyoto, Japan). L24 was synthesized exactly as described for the related peptide (LA)₁₂ by Zhang et al. (14).

Preparation of L24–POPC Membranes. The membranes used in this work were multilamellar dispersions of POPC, containing 1 mol % n-PC and various amounts of L24 from 0 to 10 mol %. Briefly, the membranes were prepared by the following method (23). Chloroform solutions of POPC ((0.3–1.0) \times 10⁻⁵ mol) and n-PC and a methanol solution of L24 were mixed, the solvent was evaporated with a stream of nitrogen gas, and then the lipid film on the bottom of a test tube was thoroughly dried under reduced pressure (\sim 0.1 mmHg) for 12 h. A buffer solution (0.1 mL of 10 mM PIPES and 150 mM NaCl, pH 7.0) was added to the dried lipid at 40 °C and was vortexed vigorously.

ESR Measurement. The L24-POPC membranes were centrifuged briefly, and the loose pellet (\sim 20% lipid w/w) was used for the ESR measurement. Dilution of the pellet did not cause any detectable changes in the results. The sample was placed in a capillary (i.d. = 0.5 mm) made of the gas-permeable polymer, TPX (24).

The T_1 's of the spin-labels were determined by analyzing the saturation—recovery signal of the central line obtained by the short-pulse saturation—recovery ESR technique (20, 25). To avoid artificial shortening in T_1 measurement, a relatively low level of observation power (8 μ W, with the

¹ Abbreviations: DMPC, dimyristoyl-L- α -phosphatidylcholine; DPPC, dipalmitoyl-L- α -phosphatidylcholine; L24, Ac-K₂L₂₄K₂-amide; P₂₄, Ac-K₂GL₂₄AK₂-amide; PC, phosphatidylcholine; n-PC, 1-palmitoyl-2-(n-doxylstearoyl)phosphatidylcholine, where n=5, 7, 10, 12, and 16; PE, phosphatidylethanolamine; P/L, peptide-to-lipid molar ratio; POPC, 1-palmitoyl-2-oleoyl-L- α -phosphatidylcholine; SLOT domain, slow oxygen-transport domain; Tempo-PC, tempocholine dipalmitoylphosphatidic acid ester; T_1 , spin—lattice relaxation time.

² In the present paper, the word "transport" is used in its basic physical sense, indicating the product of the (local) translational diffusion coefficient and the (local) concentration of oxygen in the membrane. Active transport across the membrane is not the subject of this paper.

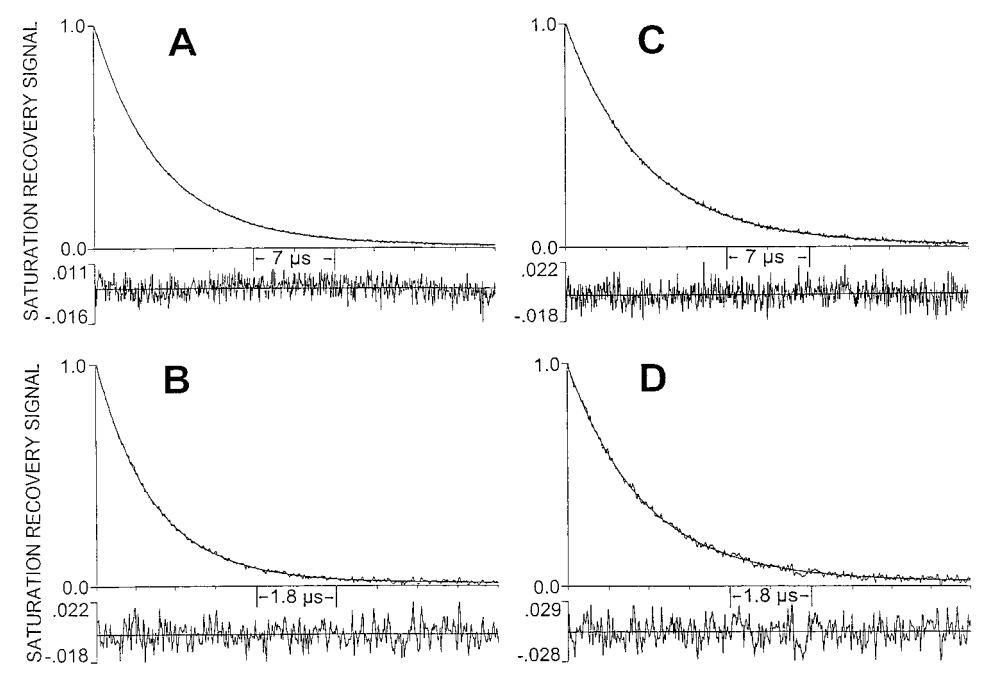


FIGURE 1: Representative saturation—recovery signals and fitted curves of 5-PC in POPC membranes in the absence (A, B) and the presence (C, D) of 1/10 (mol/mol) of L24 at 20 °C. The fast recovery curves (B, D) were obtained for samples equilibrated with a gas mixture of 50% air and 50% nitrogen gas at 20 °C, and the slow ones (A, C) were obtained in the absence of molecular oxygen for samples equilibrated with 100% nitrogen gas. The solid lines indicate the fit to single-exponential curves with time constants of 5.92 (A), 1.33 (B), 6.81 (C), and 1.69 μ s (D). The difference between experimental data and the exponential fit is shown in the lower part of each recovery curve.

loop—gap resonator delivering an H_1 field of 3.6×10^{-5} gauss) was used for all experiments. For measurements of the oxygen transport parameter, the concentration of oxygen in the sample was controlled by equilibration with the same gas that was used for the temperature control, i.e., a controlled mixture of nitrogen and dry air adjusted with flowmeters (Matheson Gas Products model 7631H-604; 18, 24).

To measure the hydrophobicity profiles across the membrane, the hyperfine interactions of the nitroxide were used. The principle and the conditions for this measurement are described in the Results. Actual measurements were carried out as follows. Briefly, the sample was placed in a 0.9 mm i.d. gas-permeable TPX capillary, and the capillary was placed inside the ESR dewar insert, which was then equilibrated with nitrogen gas used for temperature control. The sample was thoroughly deoxygenated at a temperature well above the phase transition of the lipid bilayer. The sample was then frozen (-165 °C), and the ESR spectra were obtained at the X-band. A Varian E-109 spectrometer with Varian temperature control accessories and an E-231 Varian multipurpose cavity (rectangular TE₁₀₂ mode) was used. The temperature was monitored using a copperconstantan thermocouple that was placed in the sample just above the active volume of the cavity.

RESULTS AND DISCUSSION

Measurement of T_1 in L24-POPC Membranes. Typical saturation-recovery curves for 5-PC in POPC and L24-POPC membranes (1/10) at 20 °C in the presence and absence of air are displayed in Figure 1. The recovery curves were fitted by a sum of single, double, or triple exponentials and were compared. The results indicate that, for all of the recovery curves obtained in this work, no substantial improvement in fitting was observed when the number of

Table 1: Electron Spin-Lattice Relaxation Times $(T_1$'s, in μ s) for n-PC's in L24-POPC Membranes at 20 °C in the Absence of Molecular Oxygen

L24/POPC (mol/mol)	5-PC	10-PC	16-PC
0	5.9	5.1	2.6
1/40	6.2	5.2	2.4
1/20	6.4	5.3	2.5
1/10	6.8	5.4	2.6

exponentials was increased from one, suggesting that these recovery curves can be analyzed as a single exponential. The decay time constants were determined with an accuracy of $\pm 3\%$ (Table 1).

Saturation—recovery measurements were carried out systematically, as a function of the partial pressure of oxygen in the equilibrating gas mixture, the molar ratio of peptide versus lipid (P/L), and the location of the spin-labels in the membrane (the hydrophobic region near the membrane surface with 5-PC, the inner regions of the membrane with 10-PC, and the central part of the bilayer with 16-PC). All measurements were carried out at 20 °C.

Rates of dynamical processes observed in the present investigation, i.e., the oxygen collision rate and the rate of lipid exchanges, were measured using T_1 in the absence of oxygen as a basic clock. In the absence of oxygen, the overall variation in T_1 for the three spin-labeled PC's in the membranes with P/L ratios of 0, 1/40, 1/20, and 1/10 is only a factor of 2.8, in the range of 2.4–6.8 μ s (Table 1).

Outline of the Theory for Evaluating the Oxygen Transport Parameter. To monitor the local diffusion—solubility characteristics of oxygen molecules in the membrane, the bimolecular collision rate between oxygen (a fast relaxing species) and the nitroxide spin-label (a slow relaxing species) placed at specific locations in the membrane was evaluated in terms of an oxygen transport parameter (W(x)) using a

pulse ESR spin-labeling method (18–20). W(x) is defined

$$W(x) = T_1^{-1}(\text{air}, x) - T_1^{-1}(N_2, x)$$
 (1)

where the T_1 's are the spin-lattice relaxation times of the nitroxide in samples equilibrated with atmospheric air and nitrogen, respectively. W(x) is proportional to the product of the local concentration C(x) and the local translational diffusion coefficient D(x) of oxygen (thus W(x) is called "transport" parameter) at a "depth" x in a membrane that is in equilibrium with atmospheric air:

$$W(x) = AD(x)C(x), \quad A = 8\pi p r_0 \tag{2}$$

where r_0 is the interaction distance between oxygen and the nitroxide radical spin-labels (\sim 4.5 Å; 26, 27), and p is the probability that an observable event occurs when a collision does occur³ and is very close to 1 (27, 28).

Our previous data on W in vertebrate rhodopsin, which belongs to a class of integral membrane proteins with seven transmembrane helices, showed that W in the protein (monitored at the binding site of the β -ionone of retinal) is small; it is smaller by a factor of 10-60 as compared with W in water, and by a factor of 1.1-20, and 15-100 as compared with W in L- α -dimyristoylphosphatidylcholine (DMPC) membranes in the gel and liquid-crystalline phases, respectively (29). These results strongly suggest that the passage of molecular oxygen is slow both through an α -helix and through an array of seven α-helices that are organized as in BR.

Saturation Recovery Curves Indicate Fast Mixing of the Peptide and PC in the Time Scale of 1 us. Even in the presence of atmospheric oxygen (where the bimolecular collision rate between molecular oxygen and the spin-label is much greater than T_1^{-1} in the absence of oxygen), all recovery curves could be fitted to a single exponential function. In earlier work on BR-reconstituted membranes (2), in the absence of oxygen, all recoveries followed single exponential curves. In the presence of oxygen, doubleexponential recoveries were observed in protein-rich membranes, which indicates the presence of a special lipid environment (SLOT domain, i.e., likely to be self-associated BR domain) in which oxygen transport is 5-fold smaller than in the bulk + boundary region. The residency time of the lipids in the SLOT domain was longer than 10^{-6} s, T_1 in the presence of 100% air. It was proposed that the SLOT domain consists of lipids in contact with two proteins and/ or lipids in contact with protein and boundary lipids, which persist in the BR-rich domains (slow oxygen-transport domains) during this time scale. It was concluded that molecular oxygen makes a particularly useful probe for studies of the molecular organization of protein-rich membranes.

The single exponential recoveries after the saturating pulse indicate that the lipid environment is homogeneous in terms of oxygen transport in the microsecond range as defined by T_1 in L24-POPC membranes with a P/L ratio between 0 and 1/10. Since 16–18 molecules of phosphatidylcholine

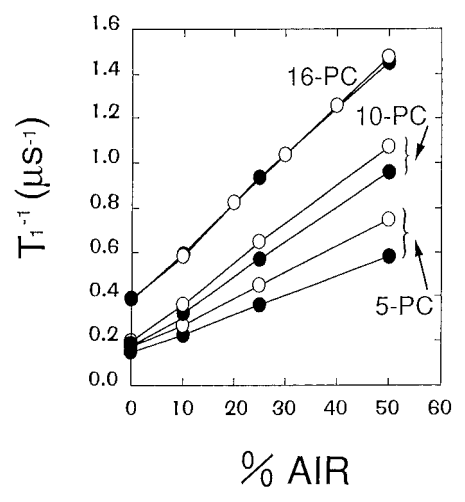


FIGURE 2: $1/T_1$ for 5-, 10-, and 16-PC in POPC (O) and L24-POPC (1/10, ●) membranes at 20 °C plotted as a function of % air (v/v) in the equilibrating gas mixture.

are required to surround a transmembrane α -helical peptide (8), L24 must form L24-rich regions at a P/L ratio of 1/10 instantaneously. Therefore, in these membranes, the presence of three different lipid environments is in principle expected: the boundary and the bulk regions, and the region in which lipids are in contact with two or more peptides, which is called the peptide-rich region in this paper. Nevertheless, the single-exponential recoveries in L24-POPC membranes suggest that the lipid exchange rate among the bulk, boundary, and peptide-rich regions is greater than the T_1 relaxation rate (greater than 3×10^6 s⁻¹, see below; cf. 30, 31). In L24-POPC membranes with any P/L ratio up to 1/10, it follows that all of the peptides are mobile and that the peptide-rich regions are forming and dispersing continually and rapidly in a time scale less than $0.3 \mu s$ (the shortest T_1 observed for the 1/10 membrane under the air atmosphere). Therefore, it is concluded that the peptiderich regions are only transiently formed in the L24-POPC membranes. Although this does not exclude the possibility of the formation of small, stable oligomers of L24, it is unlikely because L24 lacks features that would favor the formation of small, stable oligomers, while the repulsive interactions between the lysine groups work against the clustering of L24.

Membrane Profiles of the Oxygen Transport Parameter. In Figure 2, $1/T_1$ values for 5-, 10-, and 16-PC's in membranes containing either 0 or 1/10 of L24 in POPC at 20 °C are shown as a function of the oxygen concentration (in % air) in the equilibrating gas mixture. All plots of $1/T_1$ for these membranes show a linear dependence on the oxygen concentration between 0 and 50% air (Figure 2). The oxygen transport parameter, W(x), can be obtained from the slope of the linear plot (two to three decay measurements each), and the accuracy of W(x) was estimated to be better than $\pm 10\%$.

Membrane profiles of W(x) determined at three different "depths" in the membranes containing L24 at 0 and 9 mol % are shown in Figure 3. Each point was determined from the slope of the plot of $1/T_1$ vs oxygen concentration in Figure 2 and was scaled to 100% air. As shown in Figure 3, the effect of the presence of L24 on W(x) is small. The presence of L24 decreases W(x) in the membrane near the surface

³ A is remarkably independent of the hydrophobicity and viscosity of the solvent, and of the spin-label species (27, 28).

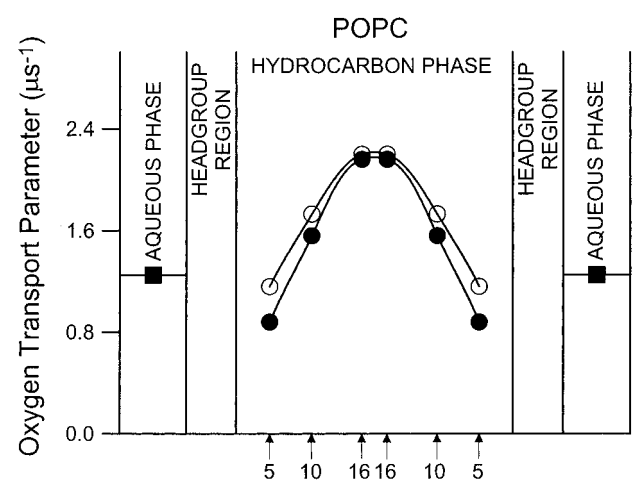


FIGURE 3: Profiles of the oxygen transport parameter, W(x), which is proportional to the product of the local concentration and the local diffusion coefficient of molecular oxygen across the hydrophobic region of various membranes. POPC (\bigcirc) and L24-POPC (1/10, \bigcirc) membranes at 20 °C. Approximate locations of the nitroxide moiety of spin-labels are indicated by arrows under the baseline. The oxygen transport parameter in the aqueous phase was obtained with 1-[^{15}N]-1-oxyl-4-oxo-2,2,6,6-tetramethylpiperidine- d_{16} , and is shown for comparison (\blacksquare).

(5-PC), but the effect becomes smaller inside the membrane, and only a slight effect of L24 can be detected in the central part of the bilayer (16-PC).

The reason why the effect of the peptide is particularly small in the central part of the membrane has yet to be determined. Other rigid transmembrane molecules such as BR (2) and polar carotenoids (32), such as zeaxanthin and violaxanthin, reduced the oxygen transport parameter W(x)at all depths in the membrane. In contrast, the effect of cholesterol on W(x) is strongly depth-dependent (19, 20). Cholesterol does not span the membrane, and the presence of cholesterol even increased W(x) in the middle of unsaturated-PC bilayers, while it decreased W(x) near the surface of the membrane. In the case of L24, complex interplay among the barrier effect of L24 for oxygen diffusion (i.e., the rate of passage through L24 is low), induction of packing defects of lipid alkyl chains, and extension of alkyl chains due to hydrophobic mismatch in length might have resulted in the small effect of L24 on W(x) in POPC membranes. In the central part of the membrane, the effect of hydrophobic mismatch would be smaller, which probably leads to a smaller effect of L24 on oxygen transport in the middle of the membrane.

Outline of Measurements of Hydrophobicity Profiles across the Membrane. As a measure of "hydrophobicity", we take advantage of the solvent effects on the hyperfine interaction (33, 34). The z component of hyperfine interaction (A_z) correlates with the static dielectric constant ϵ of the bulk solvent (34-38). The A_z values in the membrane can be related to the local dielectric constant in the membrane, which is termed "hydrophobicity" in this report (34-38). The A_z value is correlated with the local concentration of water at a given depth in the membrane, although it does not give an absolute concentration of water. Because of these relationships, the local hydrophobicity in the membrane is often compared with that of the bulk solvent (34-38).

This method is based on the dependence of unpaired electron spin density at the nitrogen nucleus on solvent polarity (23, 34, 38). Polar solvents tend to increase the unpaired electron spin density at the nitrogen atom, and therefore, to affect the hyperfine interaction between the unpaired electron spin and the nitrogen nuclear spin, particularly A_z . With an increase in solvent polarity, A_z increases. When Griffith et al. developed this method, they were the first to describe the shapes of the hydrophobicity profiles across lipid bilayer membranes (34). Using A_z as a convenient experimental observable, the water accessibility into the membrane (hydrophobicity profile) was estimated. In this method, a nitroxide free-radical moiety is placed at different depths in the lipid bilayer by attaching it to a specific carbon in stearic acid. Griffith et al. clearly demonstrated the presence of the hydrophobic barrier and its approximate shape (34).

The measurements were performed in a frozen suspension of liposomes at -165 °C. This was necessary to distinguish the solvent polarity effects from the motional effects on the spectrum. At this temperature, no appreciable molecular motion is detected on a time scale of 10^{-7} s. Under these conditions, the maximal splitting value, which can be easily read from the conventional ESR spectrum, gives $2A_z$.

The magnetic parameters (including the hyperfine interaction tensors) of spin-labels in the membrane at lower temperatures correlate well with those at physiological temperatures (36). In addition, we previously examined the accessibility of an ion into various parts of the membrane at a physiological temperature and observed a good correlation with the hydrophobicity profiles obtained at lower temperatures (37).

Hydrophobicity Profiles across L24–POPC Membranes. ESR spectra of n-PC's, where n=5, 7, 10, 12, and 16, in frozen suspensions of L24–POPC membranes lacked any sign of the presence of two components, and no L24-dependent increase of the line width (possibly due to the presence of the two components) was observed, suggesting that L24 and POPC are miscible under the conditions employed here. Therefore, A_z values can be simply determined from the ESR spectra.

Figure 4 shows the hydrophobicity profiles across these membranes. Here, the $2A_z$ data are presented as a function of the approximate position of the nitroxide moiety of the spin-label within the lipid bilayer (the width of the hydrocarbon phase and the locations of the spin probe in the stearic acid are simply scaled to the number of carbon atoms in the alkyl chain). Smaller $2A_z$ values (upward changes in the profiles) indicate higher hydrophobicity. The hydrophobicity profiles show gradual increases toward the bilayer center for all L24-POPC membranes.

Previously, we have shown that saturated-PC membranes exhibit low hydrophobicity (high polarity) across the membrane, comparable to 2-propanol and 1-octanol, even at the membrane center, where the hydrophobicity is highest (37). The introduction of a double bond at C9—C10 was found to *decrease* the level of water penetration at all locations in the membrane, and this effect is considerably greater with the *cis* configuration than with the *trans* configuration. Recently, Huster et al. found that water permeability of dioleoyl-PC membrane is smaller than that of 1-stearoyl-2-oleoyl-PC (39), indicating that addition of a double bond to

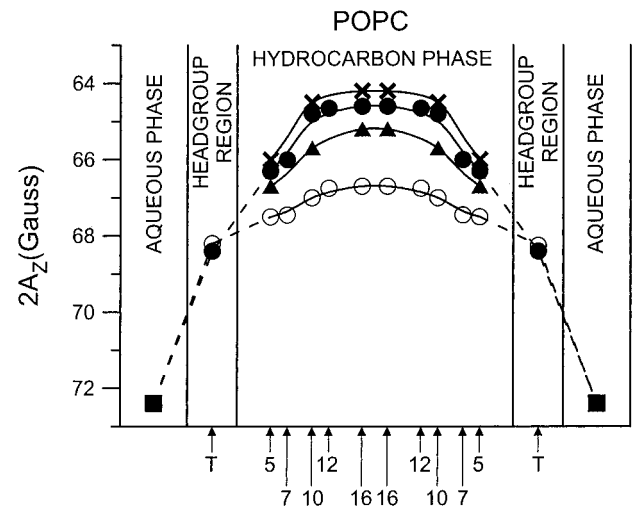


FIGURE 4: Hydrophobicity profiles $(2A_z)$ across L24—POPC membranes at P/L ratios of 0 (\bigcirc), 1/40 (\blacktriangle), 1/20 (\blacksquare), and 1/10 (\times). Data obtained with Tempo-PC and n-PC's. Upward changes indicate increases in hydrophobicity. $2A_z$ for 16-SASL in the aqueous phase (\blacksquare) was calculated from isotropic hyperfine constant of the nitroxide spin-label as described previously (Subczynski et al., 1994). Broken lines are used for connecting the points obtained with different types of the nitroxide radicals.

an alkyl chain increases hydrophobicity of the membrane, which is in agreement with our observation.

The hydrophobicity profile of the POPC membrane (without L24) shows that its features lie between those for DPPC and DOPC membranes (37). In the central part of the membrane, the hydrophobicity of POPC is close to that of 1-decanol ($\epsilon=10$), while the hydrophobicity of DPPC is like those of 2-propanol and 1-octanol ($\epsilon\sim10-20$), and DOPC is as hydrophobic as dipropylamine ($\epsilon\sim3$).

L24 (9 mol %) increases the hydrophobicity of the central part of the membrane to the level of pure hexane (as compared with 16-PC in hexane, $\epsilon \sim 2$), while the pure POPC membrane is like 1-decanol in the central part of the bilayer, as monitored by 16-PC. L24 (9 mol %) also increases the hydrophobicity at C5, from the level of 2-propanol to that of 1-decanol or *N*-butylamine. Meanwhile, L24 slightly decreased the hydrophobicity at the membrane surface, as detected with Tempo-PC, which is expected because L24 breaks the tight network of the PC headgroups

and adds polar lysine residues at the membrane-water interface.

Conventional ESR also Indicates the Presence of a Single Lipid Environment in the Time Scale of 10^{-7} s and That L24 Is Primarily Monomeric. The effect of L24 on alkyl chain order was studied at three different depths in POPC membranes. Figure 5 shows a panel of conventional ESR spectra of 5-, 10-, and 16-PC in POPC membranes containing 0 and 1/10 molar ratios of L24 to POPC at 20 °C.

A remarkable feature of these spectra is that there is no indication of the presence of two components (so-called boundary and bulk components) in the ESR spectra at any temperature and at any L24 concentration employed in the present work. This result is consistent with the oxygen transport data, in which all of the saturation—recovery curves were single-exponential curves. As we suggested in the earlier part of this paper, we propose that lateral diffusion of both L24 and POPC is fast and that the exchange rates of these molecules among the bulk, boundary, and L24 cluster regions are fast. Because only a single component is seen in the conventional ESR time scale, the exchange rate is proposed to be greater than $10^7 \, \mathrm{s}^{-1}$.

In similar experiments using BR (2), gramicidin (40), and a peptide whose sequence is the same as the transmembrane domain of epidermal growth factor receptor (unpublished observation), clear two-component spectra of the lipid spinlabels were obtained. These are thought to be due to the longer residence time of lipids in the boundary and/or self-aggregated region of these peptides and proteins; the residence time may be longer than $0.1~\mu s$.

Our conclusion that L24 is primarily monomeric in POPC bilayers is compatible with previous studies of the closely-related peptide, P₂₄, in DPPC bilayers. Both Morrow et al. (8) and Zhang et al. (13) concluded that each peptide molecule perturbs the hydrocarbon chain-melting of approximately 14–18 molecules, based on the reduction of the enthalpy of the DPPC gel to liquid crystalline phase transition observed by high-sensitivity differential scanning calorimetry. Because this range of values is very similar to the 16–18 molecules of DPPC calculated to form a single boundary layer around each P₂₄ molecule, this finding suggests that the peptide is at least primarily monomeric in this system (peptide aggregation should have reduced this value signifi-

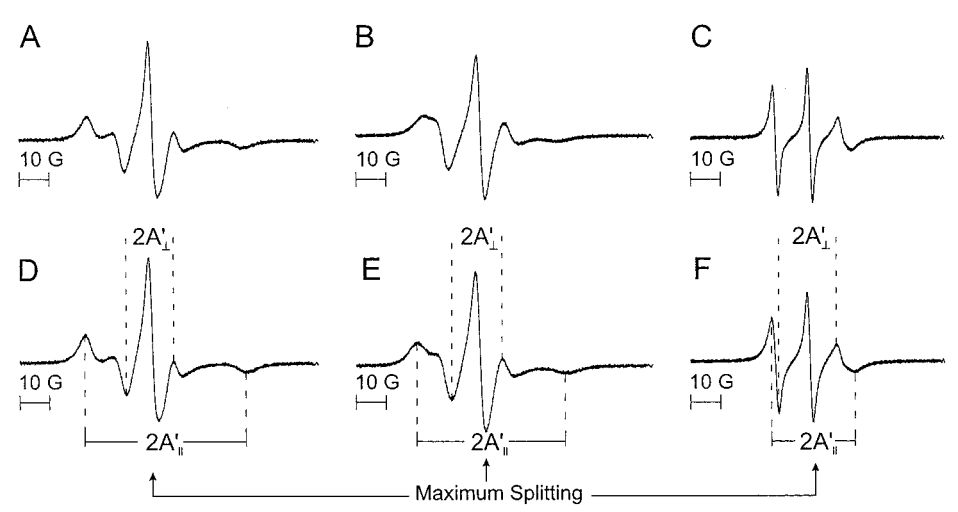


FIGURE 5: Panel of ESR spectra of 5- (A, D), 10- (B, E), and 16-PC (C, F) in POPC membranes in the absence (A, B, C) and presence (D, E, F) of L24 (1/10 mole ratio) at 20 °C.

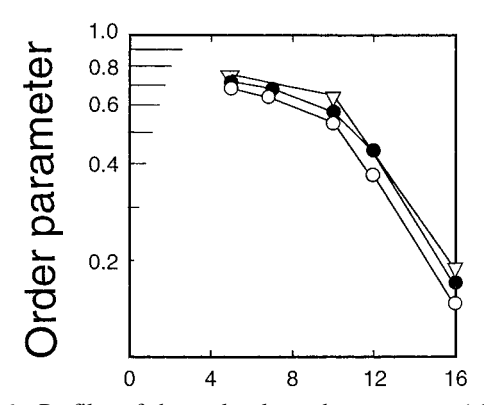


FIGURE 6: Profiles of the molecular order parameter (plotted in log scale) obtained with 5-, 7-, 10-, 12-, and 16-PC in L24-POPC membranes (0, 1/20, and 1/10 mole ratio; \bigcirc , \bullet , and ∇ , respectively) at 20 °C.

cantly). Similarly, Pauls et al. (9), using deuterium NMR spectroscopy, were able to determine that the P₂₄ molecule rotates about its long axis perpendicular to the DPPC bilayer plane, with a rotational correlation time of 2×10^{-7} s, a value expected for a monomeric α -helical peptide in a lipid bilayer of viscosity of approximately 1 P. Finally, spinlabeled L24 rotates at the rate expected of a transmembrane peptide monomer in a variety of liquid-crystalline PC model membranes (John D. Stamm and David D. Thomas, personal communication). Thus, L24 and its related peptides appear to be well dispersed in the various PC model membranes in the fluid state, even at rather high peptide concentrations, unless there is a quite large hydrophobic mismatch between the peptide and the host lipid bilayer (13, 15). This miscibility may be due primarily to the two positively charged lysine residues at each end of the peptide molecule, and perhaps secondarily to the relatively smooth hydrophobic surface minimizing the possibility of favorable peptidepeptide packing.

Effect of L24 on Alkyl Chain Order. Figure 6 shows the profiles of the order parameters obtained with 5-, 10-, and 16-PC in L24-POPC membranes at 20 °C. The order parameter S was calculated according to Marsh (41) from ESR spectra using the equation,

$$S = 0.5407(A_{\parallel}' - A_{\perp}')/a_0 \tag{3}$$

where

$$a_0 = (A_{\parallel}' + 2A_{\perp}')/3 \tag{4}$$

 A_{\parallel}' and $2A_{\perp}'$ were measured directly from the ESR spectra as shown in Figure 5. The order observed here is limited by the time averaging over 10^{-7} s, i.e., the anisotropy of magnetic interaction of the nitroxide spin-label probe, and the order parameter at the nth position shown here does not reflect the true distribution of vectors $C_{n-1} \rightarrow C_{n+1}$ along the molecular axis. The alkyl chain order increases gradually with an increase of L24 concentration in the membrane. The increase is largely proportional to the P/L ratio (between 0 and 1/10) at temperatures between 10 and 55 °C (data not shown).

Figure 7 shows the effect of L24 on the alkyl chain order, which is displayed as a function of temperature. With an increase of temperature, the alkyl chain order decreases. The addition of L24 increases the alkyl chain order at all

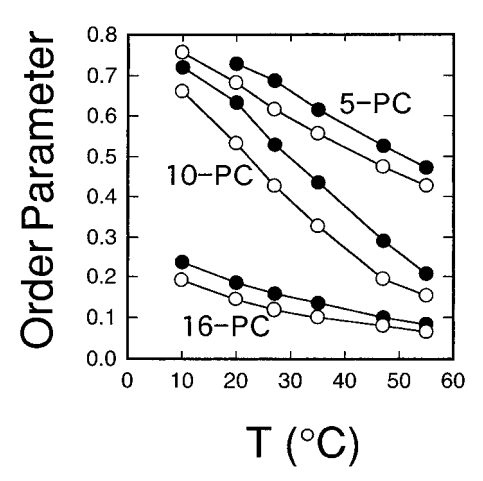


FIGURE 7: Molecular order parameters of 5-, 10-, and 16-PC in L24−POPC membranes (0 and 1/10 mole ratio; ○ and ●, respectively) plotted as a function of temperature.

temperatures. Its effect on the alkyl chain order at a ratio of 1/10 is approximately equivalent to lowering the temperature by 8 °C at all membrane depths and at all temperatures examined here. This ordering effect was also confirmed by the ESR spectra of oriented multibilayers of L24-POPC membranes (results not shown).

The observation that L24 increases the orientational order of the POPC hydrocarbon chains is compatible with the results of Davis et al. (5) and Roux et al. (10), who showed that P₂₄ and P₂₀ slightly increase the orientational order of the hydrocarbon chains of DPPC and DMPC bilayers, respectively, in the liquid-crystalline states. Similarly, using Fourier-transform infrared spectroscopy, Zhang et al. (13) showed a slight decrease in conformational disorder of the hydrocarbon chains of DPPC by P24 in liquid-crystalline DPPC bilayers. In all of these systems, as in the present one, the increase in the phospholipid hydrocarbon chain order is consistent with theories of hydrophobic mismatch (see refs 42 and 43 and references therein), since the hydrophobic length of the peptide exceeds that of the lipid hydrocarbon core in each case, resulting in a tendency of the peptide to decrease the conformational order of the hydrocarbon chain in order to increase its effective length.

It is interesting to note in this regard that natural membrane proteins typically disorder the hydrocarbon chains of the lipids with which they are in contact, as deduced by consistently interpreting the results of ²H-NMR, ESR, and FTIR spectroscopy (44-46); note that, in general, the order parameter determined spectroscopically depends on the characteristic time scale of each spectroscopic method employed. In the spin-label time scale, the apparent alkyl chain order of the lipids that are in contact with membrane proteins increases (45 and references therein).) In contrast, the incorporation of L24 and related peptides increases the orientational order of the phospholipid hydrocarbon chains, as deduced from the results of the same three spectroscopic techniques (5, 10, 13, and the present research). This qualitative difference in effect of natural proteins and L24 and related peptides on lipid hydrocarbon chain orientational order may be due to the compositional homogeneity of the model peptides, which present a molecularly smooth surface to the hydrocarbon chains of the adjacent phospholipids, in contrast to the rougher surfaces of the transmembrane

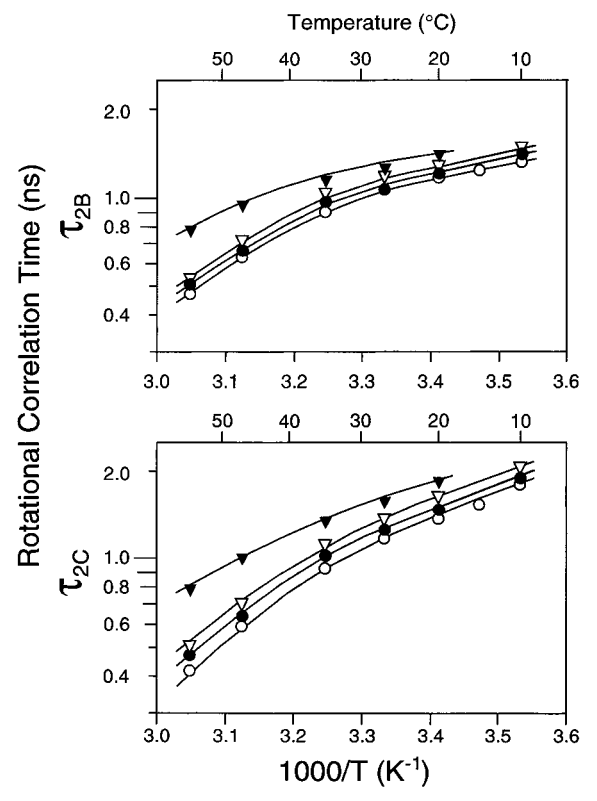


FIGURE 8: Effective rotational correlation times, τ_{2B} and τ_{2C} , of 16-PC in L24-POPC membranes at P/L ratios of 0 (\bigcirc), 1/40 (\blacksquare), 1/20 (\triangledown), and 1/10 (\blacktriangledown), plotted as a function of reciprocal temperature.

segments of the compositionally heterogeneous natural transmembrane proteins.

In reconstituted membranes of rhodopsin, under conditions of hydrophobic mismatch, (transient) oligomerization of rhodopsin was induced (42). Such oligomerization is not due to attractive interactions between rhodopsin molecules, but primarily to the fact that the rhodopsin-lipid interaction is unfavorable due to hydrophobic mismatch, as compared with lipid-lipid and rhodopsin-rhodopsin interactions. Rhodopsin molecules tend to be excluded from the lipid domains, and thus the unfavorable rhodopsin-lipid interaction was reduced. Because the association state of rhodopsin varies greatly with changes of only two methylene groups in the PC alkyl chain, it is likely to be determined by a delicate balance of the free energies of protein-protein, protein-lipid, and lipid-lipid interactions. Therefore, with the present peptide, the repulsive interactions between lysine residues probably dominate the interaction, and keep the association of L24 minimal.

Effect of L24 on 16-PC Reorientational Rate. Figure 8 shows the effective rotational correlation time of 16-PC, which was obtained by assuming isotropic rotational diffusion of the attached nitroxide (47). τ_{2B} is obtained from the linear term of the line width parameter, while τ_{2C} is obtained from the quadratic term. The closeness of these two values suggests that the isotropic approximation may be useful for the analysis of 16-PC movement. L24 decreases the effective rotational correlation time of 16-PC at all temperatures. At lower temperatures, greater differences between τ_{2B} and τ_{2C} were observed, indicating increases in the motional anisotropy of the nitroxide attached to 16-PC as the motion slows down.

Tempo-PC was used to monitor the membrane—water interfaces in this work. However, no significant changes in the presence of L24 (at 1/20 mole ratio) were detected in terms of rotational mobility, oxygen transport, and hydrophobicity.

CONCLUSIONS

- (1) Both L24 and POPC are likely to be undergoing fast translational diffusion in L24–POPC membranes of P/L ratios up to 1/10. The exchange rates of these molecules among the bulk, boundary, and L24 cluster regions are fast. L24 must form peptide-rich regions at a P/L ratio of 1/10, but the peptide-rich regions form and disperse rapidly on a time scale shorter than 0.1 μ s. In addition, it is unlikely that L24 forms small, stable oligomers, based on its molecular structure and positive charges.
- (2) The effect of the presence of L24 on oxygen transport in POPC membranes is small, which should be contrasted with the large effect of BR. The presence of L24 decreases W(x) in the POPC membrane near the surface (5-PC), but the effect becomes smaller inside the membrane, and only a slight effect of L24 can be detected in the central part of the bilayer (16-PC).
- (3) Lateral variations of hydrophobicity were not found in POPC membranes containing up to 9 mol % L24. L24 increases the hydrophobicity of the central part of the POPC membrane to the level of pure hexane (as monitored with 16-PC), while the central part of the pure POPC membrane bilayer is like 1-decanol. L24 also increases the hydrophobicity at C5, from the level of 2-propanol to that of 1-decanol or *N*-butylamine.
- (4) Even after the addition of L24 up to 9 mol %, the conventional ESR spectra of all PC spin-labels at all temperatures indicated the presence of a single lipid environment. The addition of 9 mol % L24 changes the order parameter profile in the same way as simply decreasing the temperature by ${\sim}8$ °C at all temperatures studied in this work.

REFERENCES

- Kusumi, A., and Sako, Y. (1996) Curr. Opin. Cell Biol. 8, 566-574.
- Ashikawa, I., Yin, J.-J., Subczynski, W. K., Kouyama, T., Hyde, J. S., and Kusumi, A. (1994) *Biochemistry* 33, 4947–4952.
- Sheetz, M. P. (1993) Annu. Rev. Biophys. Biomol. Struct. 22, 417–431.
- 4. Singer, S. J., and Nicholson, G. L. (1972) *Science 175*, 720–731
- Davis, J. H., Clare, D. M., Hodges, R. S., and Bloom, M. (1983) Biochemistry 22, 5298-5305.
- Huschilt, J. C., Hodges, R. S., and Davis, J. H. (1985) Biochemistry 24, 1377–1386.
- Huschilt, J. C., Millman, B. M., and Davis, J. H. (1989) Biochim. Biophys. Acta. 979, 139–141.
- 8. Morrow, M. R., Huschilt, J. C., and Davis, J. H. (1985) *Biochemistry* 24, 5396–5406.
- Pauls, K. P., MacKay, A. L., Soderman, O., Bloom, M., Tanjea, A. K., and Hodges, R. S. (1985) *Eur. Biophys. J.* 12, 1–11.
- 10. Roux, M. R., Neumann, J. M., Hodges, R. S., Devaux, P. F., and Bloom, M. (1989) *Biochemistry* 28, 2313–2321.
- Bolen, E. J., and Holloway, P. W. (1990) Biochemistry 29, 9638–9643.

- Zhang, Y.-P., Lewis, R. N. A. H., Hodges, R. S., and McElhaney, R. N. (1992) *Biochemistry 31*, 11572–11578.
- Zhang, Y.-P., Lewis, R. N. A. H., Hodges, R. S., and McElhaney, R. N. (1992) *Biochemistry 31*, 11579–11588.
- Zhang, Y.-P., Lewis, R. N. A. H., Henry, G. D., Sykes, B. D., Hodges, R. S., and McElhaney, R. N. (1995) *Biochemistry* 34, 2348–2361.
- Zhang, Y.-P., Lewis, R. N. A. H. Hodges, R. S., and McElhaney, R. N. (1995) *Biochemistry* 34, 2362–2371.
- Zhang, Y.-P., Lewis, R. N. A. H., Hodges, R. S., and McElhaney, R. N. (1995) *Biophys. J.* 68, 847–857.
- Axelsen, P. H., Kaufman, B. K., McElhaney, R. N., and Lewis, R. N. A. H. (1995) *Biophys. J.* 69, 2770–2781.
- Kusumi, A., Subczynski, W. K., and Hyde, J. S. (1982) Proc. Natl. Acad. Sci. U.S.A. 79, 1854–1858.
- Subczynski, W. K., Hyde, J. S., and Kusumi, A. (1989) Proc. Natl. Acad. Sci. U.S.A. 86, 4474

 –4478.
- Subczynski, W. K., Hyde, J. S., and Kusumi, A. (1991) *Biochemistry* 30, 8578–8590.
- Pasenkiewicz-Gierula, M., Subczynski, W. K., and Kusumi, A. (1991) *Biochimie 73*, 1311–1316.
- Pace, R. J., and Chan, S. I. (1982) J. Chem. Phys. 76, 4241
 4247
- Kusumi, A., Subczynski, W. K., Pasenkiewicz-Gierula, M., Hyde, J. S., Merkle, H. (1986) *Biochim. Biophys. Acta* 854, 307–317.
- 24. Hyde, J. S., and Subczynski, W. K. (1989) in *Biological Magnetic Resonance*, Vol. 8, Spin Labeling: Theory and Applications (Berliner, L. J., and Reuben, J., Eds.) pp 399–425, Plenum, New York.
- Yin, J.-J., Pasenkiewicz-Gierula, M., and Hyde, J. S. (1987) *Proc. Natl. Acad. Sci. U.S.A.* 79, 1854–1858.
- Subczynski, W. K., and Hyde, J. S. (1981) *Biochim. Biophys. Acta.* 643, 283–291.
- Hyde, J. S., and Subczynski, W. K. (1984) J. Magn. Reson. 56, 125-130.
- 28. Subczynski, W. K., and Hyde, J. S. (1984) *Biophys. J.* 45, 743–748.
- Subczynski, W. K., Renk, G., Crouch, R., Hyde, J. S., and Kusumi, A. (1992) *Biophys. J.* 63, 573–577.

- East, J. M., Melville, D., and Lee, A. G. (1985) Biochemistry 24, 2615–2623.
- 31. Ryba, N. J. P., Horváth, L. I., Watts, A., and Marsh, D. (1987) *Biochemistry* 26, 3234–3240.
- 32. Subczynski, W. K., Markowska, E., and Sielewiesiuk, J. (1991) *Biochim. Biophys. Acta 1068*, 68–72.
- 33. Windle, J. J. (1981) J. Magn. Reson. 45, 432-439.
- 34. Griffith, O. H., Dehlinger, P. J., and Van, S. P. (1974) *J. Membr. Biol.* 15, 159–192.
- 35. Johnson, M. E. (1981) Biochemistry 20, 3319-3328.
- Kusumi, A., and Pasenkiewicz-Gierula, M. (1988) Biochemistry 27, 4407–4415.
- Subczynski, W. K., Wisniewska, A., Yin, J.-J., Hyde, J. S., and Kusumi, A. (1994) *Biochemistry* 33, 7670-7681.
- 38. Griffith, O. H., and Jost, P. C. (1976) in *Spin Labeling: Theory and Applications* (Berliner, L. J., Ed.) pp 453–523, Academic Press, New York.
- Huster, D., Jin, A. J., Arnold, K., and Gawrisch, K. (1997) *Biophys. J.* 73, 855–864.
- Wisniewska, A., and Subczynski, W. K. (1996) Curr. Top. Biophys. 20, 86–92.
- 41. Marsh, D. (1981) in *Membrane Spectroscopy* (Grell, E., Ed.) pp 51–142, Springer-Verlag, Berlin.
- Kusumi, A., and Hyde, J. S. (1982) Biochemistry 21, 5978
 – 5983.
- 43. Sperotto, M. M., and Mouritsen, O. G. (1991) *Biophys. J.* 59, 261–270.
- 44. Bloom, M., and Smith, I. C. P. (1985) in *Progress in Protein—Lipid Interactions* (Watts, A., and DePont, J. J. H. H. M., Eds.) Vol. 1, pp 61–88, Elsevier, Amsterdam.
- 45. Marsh, D. (1997) Eur. Biophys. J. 26, 203-208.
- 46. Mendelsohn, R., and Mantsch, H. H. (1986) in *Progress in Protein—Lipid Interactions* (Watts, A., and DePont, J. J. H. H. M., Eds.) Vol. 2, pp 103–146, Elsevier, Amsterdam.
- 47. Berliner, L. J. (1978) *Methods Enzymol.* 49, 466–470. BI972148+